Rotational and intrinsic states above the $K^\pi = 25/2^-$, $T_{1/2} = 25$ day isomer in ^{179}Hf

S. M. Mullins, G. D. Dracoulis, A. P. Byrne,* T. R. McGoram, S. Bayer, R. A. Bark, R. T. Newman,† W. A. Seale,‡ and F. G. Kondev§

Department of Nuclear Physics, RSPhysSE, The Australian National University, Canberra, ACT 0200, Australia
(Received 29 October 1999; published 10 March 2000)

Time-correlated, particle-tagged γ spectroscopy of the stable nucleus ^{179}Hf was undertaken with incomplete fusion reactions initiated by beams of ^{9}Be and ^{7}Li incident on targets of ^{176}Yb. Intrinsic and rotational states above the three-quasiparticle $K^\pi = 25/2^-$, $T_{1/2} = 25$ day isomer, ^{179}Hf^{m2}, are reported. The rotational band based on ^{179}Hf^{m2} has $g_K - g_R$ values that are consistent with the previously suggested $\nu 9/2^+ \otimes \pi^2 [7/2^+, 9/2^-]$ configuration assignment. A value of $g_R = 0.34(5)$ was derived for the collective g factor of ^{179}Hf^{m2}, which is considerably higher than that found for the $9/2^+$ ground state. The difference is consistent with a reduction of the proton pairing strength due to blocking in the $K^\pi = 25/2^-$ $\nu \otimes \pi^2$ configuration. A number of $\nu^3 \pi^2$ five-quasiparticle configurations were identified, the highest of which is an yrast $K^\pi = 43/2^+$, $T_{1/2} = 15(5)$ μs isomer. It decays to an yrast $K^\pi = 39/2^-$ state, which in turn decays to a rotational band based on a $K^\pi = 33/2^-$ state. The $K^\pi = 33/2^-$ state decays to the rotational band associated with ^{179}Hf^{m2}. Semiempirical calculations reproduce the excitation energies of the three- and five-quasiparticle states above ^{179}Hf^{m2} to within ~ 200 keV. The calculations predict that the lowest seven-quasiparticle state will arise from a $\nu^5 \pi^2$ configuration with $K^\pi = 47/2^-$, which is just beyond the maximum spin accessible with the reactions employed here.

PACS number(s): 27.70.+q, 23.20.Lv, 21.10.Re, 21.60.Ev

I. INTRODUCTION

In an axially symmetric deformed nucleus, the total angular momentum operator (**J**) and its component (**J**$_z$) along the symmetry axis both commute with the Hamiltonian of the system. Hence, the eigenvalues associated with each operator (namely, J and K, respectively) are both good quantum numbers. This has particular significance in the $A = 180$ region of prolate-deformed nuclei, where multiquasiparticle states with large K values are common. The large K values arise because many of the single-particle orbitals which make up the multiquasiparticle states themselves have large angular momentum projections (Ω) on the nuclear symmetry axis. Electromagnetic transitions between high-K states are in principle forbidden if the change in K is greater than the multipolarity of the photon. In practice, transitions proceed due to admixtures of other K values into one or both of the states, though the decay is often severely retarded. Hence, the approximate conservation of the K quantum number can lead to metastable (''isomeric'') behavior for many states which are based on high-K, multiquasiparticle configurations.

A number of multiquasiparticle states in the heaviest stable hafnium nuclei are so highly favored that they can only decay via low-energy, high-multipolarity γ-ray transitions, so that they are also ''spin traps,'' as well as K isomers. This can result in some remarkably long half-lives. A prime example is the $K^\pi = 25/2^-$ three-quasiparticle state at 1106 keV in ^{179}Hf [1,2], which has a half-life of 25 days [3]. The decay and magnetic moment [4] of this isomer (sometimes referred to as ^{179}Hf^{m2}) have been studied, but excited states above it, in particular its associated rotational band, have not been reported, since it is difficult to populate ^{179}Hf at sufficiently high angular momentum. This is because the only conventional (HI,xn) fusion-evaporation reaction that is available is ^{176}Yb(α,n)^{179}Hf. Though this reaction has been used to produce samples of ^{179}Hf^{m2} [1,2], it would not be expected to lead to a strong population of states above ^{179}Hf^{m2}.

In the measurements reported here, incomplete fusion or ''breakup'' reactions, were employed to populate states up to $\sim 22\hbar$ in ^{179}Hf, and thus enabled the level structure above ^{179}Hf^{m2} to be studied for the first time. These states include the rotational band based on ^{179}Hf^{m2}, which allows an independent characterization of the isomeric configuration via the in-band branching ratios. In addition, four new three-quasiparticle states were found, and placed relative to ^{179}Hf^{m2} with the aid of time-correlated γ-γ coincidences. It was possible to make configuration assignments to two of these states from the characteristics of their associated rotational bands. Furthermore, a number of five-quasiparticle states were identified. Configuration assignments were made from a comparison with multiquasiparticle calculations that included configuration-dependent blocking of pairing correlations and residual orbital-orbital interactions. A rotational band was established on one of these states, and its branching ratios agreed with those expected for the assigned configuration.

---

*Joint appointment with the Department of Physics, The Faculties, The Australian National University, Canberra, ACT 0200, Australia.

†Permanent address: National Accelerator Center, Faure, South Africa.

‡Permanent address: Laboratório Pelletron, Departamento de Física Nuclear, Instituto de Física, Universidade de São Paulo, São Paulo, Brazil.

§Present address: Argonne National Laboratory, Argonne, IL 60439.
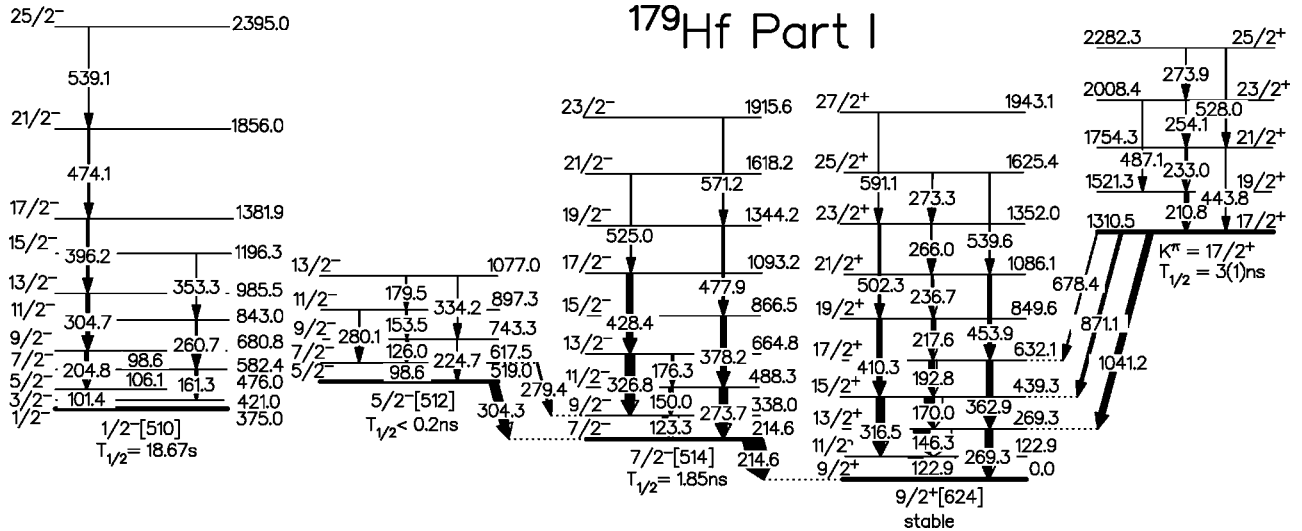
FIG. 1. Partial level scheme for ^{179}Hf in which one-quasineutron states and associated rotational bands are shown. Also shown is the proposed $K^{\pi}=17/2^{+}$ three-quasiparticle state which decays to the ground-state band.

II. EXPERIMENTAL TECHNIQUES

The measurements were performed with beams of ^{9}Be and ^{7}Li ions provided by the ANU 14UD Pelletron accelerator. Self-supporting metallic foils of ^{176}Yb, isotopically enriched to 96%, were used as targets. The ^{9}Be beams were continuous and delivered at energies of 55, 45, and 38 MeV. The nominal target thickness was 4.6 mg/cm^2 for the 55 MeV measurement, while a thinner target of 2 mg/cm^2 was used for the two lower beam energies. States in ^{179}Hf were populated via the $\alpha2n$ exit channel, where the α-particle yield came mainly from breakup of the beam. This process is known as ''incomplete fusion'' or ''massive transfer'' [5–7], and is believed to occur for collisions localized forward of the grazing angle. To first order, the reaction mechanism can be considered as breakup into α + ''^{5}He,'' followed by fusion and evaporation of the form ^{176}Yb(''^{5}He,''$2n)^{179}$Hf.

The ^{7}Li+^{176}Yb reaction populated states in ^{179}Hf via three possible exit channels, namely, $p3n$, $d2n$, and tn. The yield of ^{179}Hf (and ^{178}Hf) was found to be similar to that of ^{175}Lu and ^{176}Lu, which were populated via $\alpha4n$ and $\alpha3n$ emission, respectively [8]. Particle-tagged γ-γ coincidence data were acquired at 50 MeV with continuous beams. Delayed γ-γ coincidences were measured at a beam energy of 45 MeV where the beam was chopped with on/off periods of 11/324 μs.

The ANU Particle Detector Ball (PDB) is an array of 14 fast/slow plastic scintillators which covers $\sim$85% of 4π and detects charged particles using the phoswich technique [9]. It was placed around the target position at the center of the CAESAR γ-ray array [10]. All γ-γ coincidences within 856 ns of the detected charged particle were recorded. Particle-γ measurements were also undertaken at 55 and 45 MeV with the ^{9}Be beam.

In order to reduce the amount of scattered beam incident on the front particle detectors, they were screened with $\sim$46 mg/cm^2 Al absorber foils for the measurement made at E_{Be}=55 MeV. The 45 and 38 MeV measurements em-

ployed a thick Al disk ($\sim$160 mg/cm^2) of diameter 16 mm, as did the ^{7}Li measurements, which reduced the active solid angle of the front detectors by about 50%.

It was also found useful to analyze some archived data that were obtained from the ^{9}Be+^{176}Yb reaction at 40 MeV, where time-correlated coincidences were measured with the CAESAR array with a beam that was bunched into nanosecond pulses separated by 864 ns [11]. A number of weakly populated low-spin states were found that were not observed in the particle-tagged data.

III. DATA REDUCTION AND ANALYSIS

A. Level scheme and intensity ratios

The level scheme for ^{179}Hf is shown in three parts for clarity. In Figs. 1 and 2, the one-quasineutron states are shown, together with some three-quasiparticle states that decayed to the ground-state band. The higher spin structure proposed to reside above the $K^{\pi}=25/2^-$ metastable state is presented in Fig. 3. All transitions above this state were decoupled from the rest of the level scheme, due to the long lifetime of the isomer. In the analysis of the E_{Be}=55 MeV data, the assignment of these transitions to ^{179}Hf was guided by the dependence of the relative γ-ray intensity on whether the α particle was detected in the front, middle, or back elements of the particle detector ball, since, as discussed in previous publications [12–14], this shows an empirical correlation with the relative yield of a particular isotope. The angular dependence of the relative yield also changed with the bombarding energy, probably due to the dependence of the grazing angle on the latter. It was found that the α-particle yield associated with ^{179}Hf was strongly forward peaked at 55 MeV, so front-gated and middle/back-gated matrices were produced. Coincidence intensities for known bands in ^{177}Hf [15–17], ^{178}Hf [18], and ^{179}Hf [19] were extracted from the two matrices. A ratio of the γ-γ coincidence intensities of the form $R_{55}(F/MB)$ was generated to
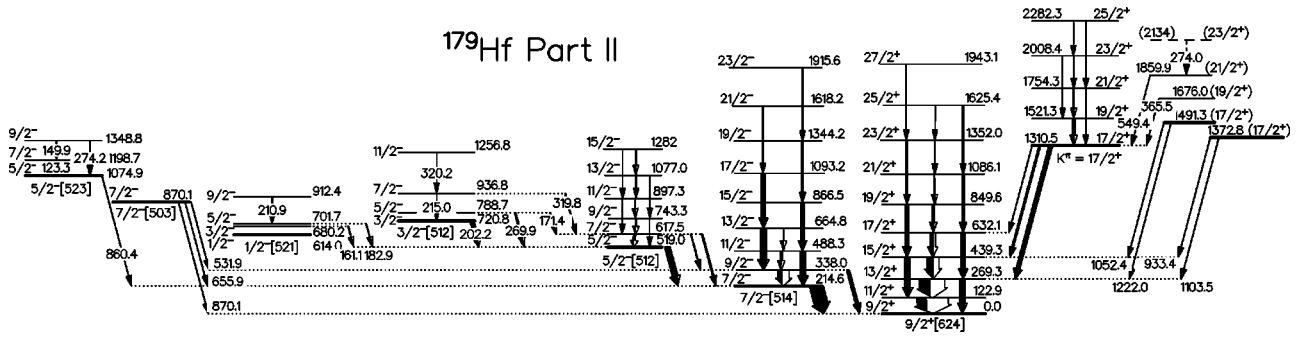
FIG. 2. Partial level scheme for ^{179}Hf in which states that were only observed in the 38 MeV α-γ-γ and 40 MeV nanosecond-pulsed γ-γ data are shown. These states arise from nonyrast one-quasineutron orbitals and possible three-quasiparticle structures, one of which may be a higher-lying $K^{\pi}=17/2^{+}$ configuration.

aid with the assignment of new bands that could not be connected to the known level schemes in either prompt or delayed coincidence. The results are shown in Fig. 4(a). The low yield of ^{179}Hf in the middle-back matrix relative to that in the forward matrix resulted in poorer statistical accuracy for the ^{179}Hf $R_{55}(F/MB)$ intensity ratios when compared to those for ^{178}Hf and ^{177}Hf.

At $E_{Be}=45$ MeV, the ratio of ^{179}Hf to ^{178}Hf was found to be essentially the same for both the front-gated and middle-gated matrices, so they were added together. The back-gated matrix contained a higher fraction of events associated with ^{178}Hf, but though a ''$R_{45}(FM/B)$'' ratio showed separation of lower spin transitions in ^{179}Hf and ^{178}Hf, it found to be of little use in the cross-check of the assignment of new high-spin transitions to ^{179}Hf. This could have been due to the effect of the absorber disk which stopped the most forward-peaked α particles. Instead, a

''$R(FM45/F55)$'' ratio [Fig. 4(b)] showed separation between ^{179}Hf and ^{178}Hf for the entire spin range, which provided unambiguous confirmation of the assignments made on the basis of the $R_{55}(F/MB)$ ratios.

At $E_{Be}=38$ MeV, the beam energy was just above the Coulomb barrier ($V_{coul}\simeq36$ MeV), and there was no measurable α-particle yield in the front elements of the particle detector ball. Hence a middle/back-gated matrix was produced, and these data were essentially pure in ^{179}Hf, which allowed the observation of a number of weak transitions from low-spin, nonyrast states.

Five new rotational bands were found, only one of which decayed to known states in ^{179}Hf. The other four did not show coincidences with known lines in any of the hafnium isotopes that were present in the data. All four bands were weakly populated in the 55 MeV middle-back matrix, which hampered the extraction of reliable $R_{55}(F/MB)$ intensity ra-
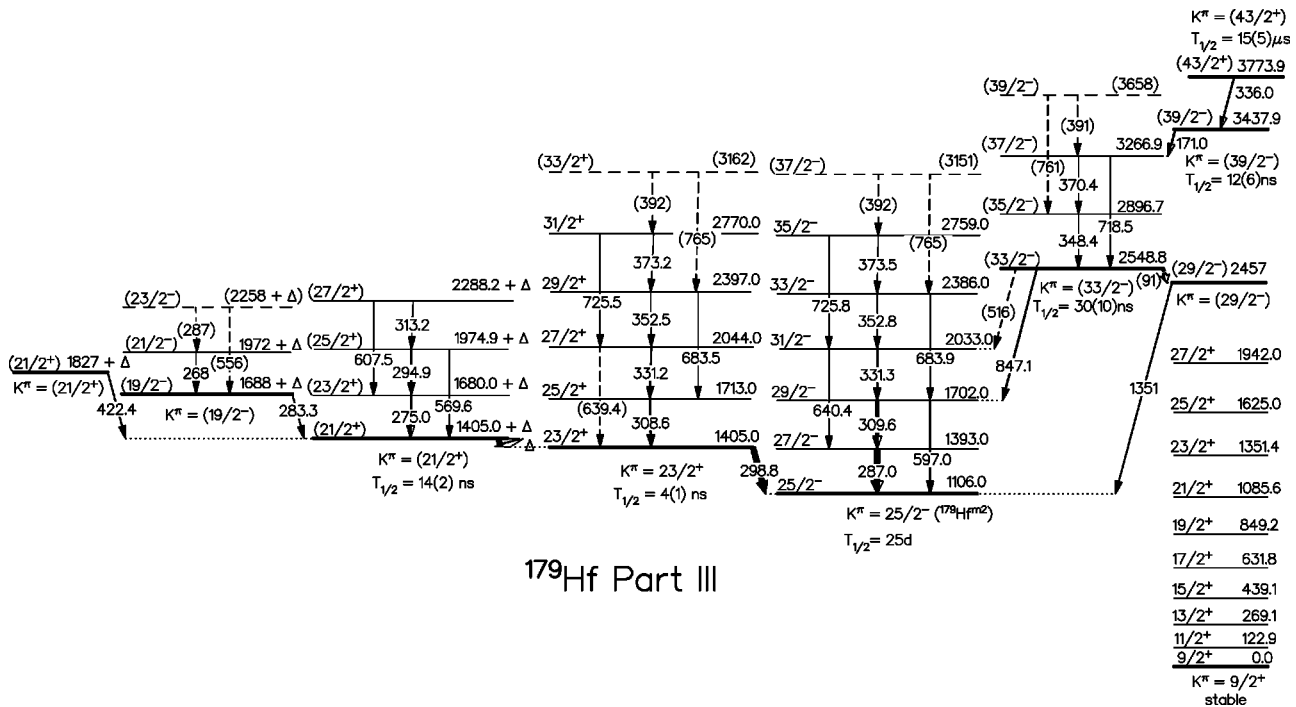
FIG. 3. Partial level scheme for ^{179}Hf in which states above the $K^{\pi}=25/2^{-}$, $T_{1/2}=25$ day isomer are shown. The levels of the ground-state band are shown to provide an energy scale.
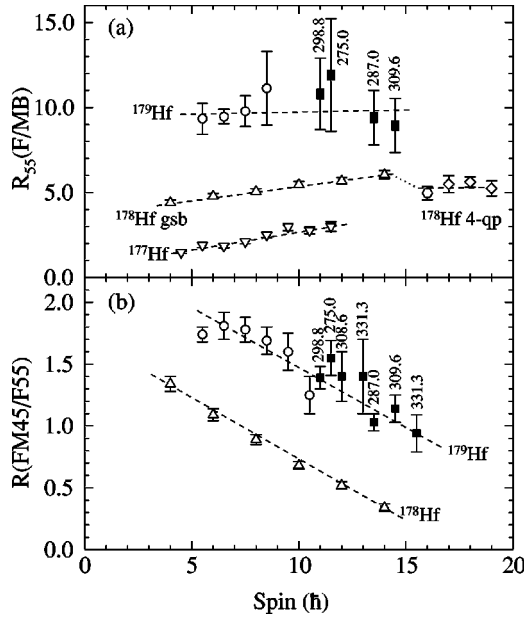
FIG. 4. (a)''Forward/middle-back'' at 55 MeV intensity ratios (see text) for γ-γ coincidences within known bands in ^{177}Hf, ^{178}Hf, and ^{179}Hf (open symbols), together with those for transitions above the $K^{\pi}=25/2^-$ three-quasiparticle isomeric state in ^{179}Hf (solid symbols, labeled by transition energy in keV). (b) $FM45/F55$ intensity ratios for ^{179}Hf and ^{178}Hf.

tios, but clearly suggested that they should all be assigned to ^{179}Hf. One band was populated with twice the intensity (in the forward-gated matrix) of the strongest of the other three (see Table I). In Fig. 4(a) this band is represented by solid symbols that correspond to the 287.0 and 309.6 keV transitions. The $R_{55}(F/MB)$ ratios clearly show that the band belongs to ^{179}Hf, and due to its intensity, it has been assigned to the $K^{\pi}=25/2^-$ isomer, since this state is yrast by ~ 500 keV. The assignment to ^{179}Hf is confirmed by the $R(FM45/F55)$ ratios shown in Fig. 4(b). A coincidence spectrum gated by the 287.0 keV transition is shown in Fig. 5(a). The spectrum shows members of the rotational band assigned to the $K^{\pi}=25/2^-$ state, but there are also transitions that belong to another band which decays via an 847.1 keV transition. The two remaining bands are both in coincidence with the 298.8 keV transition, which is assigned to ^{179}Hf on the basis of its intensity ratios. A coincidence spectrum gated by the 298.8 keV transition is shown in Fig. 5(b), where members of both bands can be seen.

B. Branching ratios and angular distributions

The well-known rotational model formulas were used to calculate values of $(g_K-g_R)/Q_0$ from the observed γ-ray branching ratios. Branching ratios do not determine the sign of $(g_K-g_R)/Q_0$, but it can be defined through γ-ray angular anisotropies which depend on both the sign and the magnitude of the mixing ratios of the $\Delta J=1$ cascade transitions. In the present cases, the particle-γ data were used to determine the sign of the A_2 coefficient where possible, from a fit to three-point angular distributions. If the collective moments g_R and Q_0 are known, then the intrinsic g factor g_K can be

obtained. Since no significant changes in quadrupole deformation are expected between the ground and multiquasiparticle states, the same value of Q_0 was used for all bands. This was taken from the measured quadrupole moment of the $9/2^+$ ground state, namely, 3.79(3) e b [20] which corresponds to $Q_0=6.95(6)$ e b. The extracted g_K factors are shown in Table II.

IV. ROTATIONAL BANDS AND CONFIGURATION ASSIGNMENTS

A. One-quasineutron configurations

The one-quasineutron intrinsic states presented in Figs. 1 and 2 had all been observed in previous light-ion transfer studies by other investigators [21–24] and in the β^- decay of ^{179}Lu [25]. Some of the rotational levels based on these intrinsic states had also been previously observed; additional higher-spin levels were found in the present work, and for the sake of completeness are reported briefly below.

1. $9/2^+[624]$ ground state

The band based on the stable $9/2^+$ ground state had been previously observed up to the $21/2^+$ state from the decay of ^{179}Hf^{m2}. It has been extended to its $27/2^+$ state in the present data. Negative A_2 values were found for the strongest $\Delta J=1$ cascade transitions, which imply negative mixing ratios. Hence, the negative sign was taken for $(g_K-g_R)/Q_0$. The value of $g_K=-0.22(4)$ is in good agreement with the Nilsson model estimate, in contrast with the analogous band in the isotone ^{181}W. This suggests that the K mixing is not as strong in ^{179}Hf as it is in ^{181}W. A similar conclusion was reached for the $9/2^+$ bands in the $N=105$ isotones ^{177}Hf and ^{179}W. This may reflect a more negative β_4 deformation in the W isotopes [26] when compared to their Hf isotopes [23], since this distortion leads to an energy compression of the $i_{13/2}$ orbital ''fan,'' which mediates greater K mixing.

2. $7/2^-[514]$ state at 214 keV

The band based on the $7/2^-$ first excited state was extended to its $23/2^-$ member, whereas it had been previously observed only to the $11/2^-$ state. Since $g_K\simeq g_R$ for this configuration, the $B(M1)$ strength is very weak, and the $\Delta J=1$ cascade transitions are not observed above the $13/2^-$ level.

3. $1/2^-[510]$ state at 375 keV

The $1/2^-$ state that arises from the $1/2^-[510]$ neutron orbital is isomeric, with a half-life of 18.67 s, since it can only decay to the $7/2^-$ state via an $M3$ transition. The band based on this state had been previously established to its $9/2^-$ state from light-ion transfer studies, but it was possible to observe the decay from the $25/2^-$ member in the present data.

4. $5/2^-[512]$ state at 519 keV

The first three levels of this band had been assigned from the light-ion transfer data. It was observed to its $15/2^-$ mem-

TABLE I. Measured and derived quantities for γ-ray transitions in ^{179}Hf. All intensities taken from 55 MeV ^{9}Be particle-γ-γ data except where noted. All A_2 values taken from 55 MeV particle-γ data.

E_γ (keV)	E_{level} (keV)	I_γ	A_2/A_0	$(J_i^\pi,K_i)\rightarrow(J_f^\pi,K_f)$
(91)	2548.8			$(33/2^-,33/2)\rightarrow(29/2^-,29/2)$
97.7	680.8	0.2(1)		$9/2^-,1/2\rightarrow7/2^-,1/2$
98.6	617.5	1.2(1)		$7/2^-,5/2\rightarrow5/2^-,5/2$
101.4	476.0	5.0(5)		$5/2^-,1/2\rightarrow1/2^-,1/2$
106.1	582.4	1.2(3)		$7/2^-,1/2\rightarrow5/2^-,1/2$
122.9	122.9	50.8(1.3)	$-0.32(4)$	$11/2^+,9/2\rightarrow9/2^+,9/2$
123.3	338.0	8.6(4)		$9/2^-,7/2\rightarrow7/2^-,7/2$
123.3	1198.7	2(1) [a]		$(7/2^-,5/2)\rightarrow(5/2^-,5/2)$
126.0	743.6	1.2(1)		$9/2^-,5/2\rightarrow7/2^-,5/2$
146.3	269.2	27.9(1.1)	$-0.37(6)$	$13/2^+,9/2\rightarrow11/2^+,9/2$
149.9	1348.8	0.5(3) [a]		$(9/2^-,5/2)\rightarrow(7/2^-,5/2)$
150.0	488.3	2.8(2)		$11/2^-,7/2\rightarrow9/2^-,7/2$
153.5	897.3	0.7(1)		$11/2^-,5/2\rightarrow9/2^-,5/2$
161.1	680.2	4.6(4) [a]		$(3/2^-,1/2)\rightarrow5/2^-,5/2$
161.3	582.4	0.9(7)		$7/2^-,1/2\rightarrow3/2^-,1/2$
170.0	439.3	16.4(6)	$-0.40(10)$	$15/2^+,9/2\rightarrow13/2^+,9/2$
171.0	3437.9	5(1) [b]		$(39/2^-,39/2)\rightarrow(37/2^-,37/2)$
171.4	788.7	1.6(3) [a]		$(5/2^-,3/2)\rightarrow7/2^-,5/2$
176.3	664.8	0.1(1)		$13/2^-,7/2\rightarrow11/2^-,7/2$
179.5	1077.0	0.5(1)		$13/2^-,5/2\rightarrow11/2^-,5/2$
182.9	701.7	2.0(3) [a]		$5/2^-,1/2\rightarrow5/2^-,5/2$
192.8	632.1	8.3(4)	$-0.18(15)$	$17/2^+,9/2\rightarrow15/2^+,9/2$
202.2	721.1	6.8(1) [a]		$3/2^-,3/2\rightarrow5/2^-,5/2$
204.8	680.8	3.8(4)		$9/2^-,1/2\rightarrow5/2^-,1/2$
207.2	1282.2	0.5(3) [a]		$(15/2^-,5/2)\rightarrow(13/2^-,5/2)$
210.9	1521.3	4.4(3)		$19/2^+,17/2\rightarrow17/2^+,17/2$
210.9	912.4	2.2(4) [a]		$(9/2^-,1/2)\rightarrow(5/2^-,1/2)$
214.6	214.6	34.1(9)	$-0.29(15)$	$7/2^-,7/2\rightarrow9/2^+,9/2$
215	788.7	0.1(1) [a]		$(7/2^-,3/2)\rightarrow3/2^-,3/2$
217.6	849.6	4.7(3)		$19/2^+,9/2\rightarrow17/2^+,9/2$
224.7	743.6	0.4(1)		$9/2^-,5/2\rightarrow5/2^-,5/2$
232.9	1754.3	1.9(2)		$21/2^+,17/2\rightarrow19/2^+,17/2$
236.7	1086.1	2.0(2)		$21/2^+,9/2\rightarrow19/2^+,9/2$
254.3	2008.4	0.4(1)		$23/2^+,17/2\rightarrow21/2^+,17/2$
260.7	843.0	1.7(3)		$11/2^-,1/2\rightarrow7/2^-,1/2$
266.0	1352.0	1.0(1)		$23/2^+,9/2\rightarrow21/2^+,9/2$
268	$1972+\Delta$	0.4(1)		$(21/2^-,19/2)\rightarrow(19/2^-,19/2)$
269.3	269.3	11.0(1)	0.23(13)	$13/2^+,9/2\rightarrow9/2^+,9/2$
269.9	788.7	3.1(5) [a]		$(5/2^-,3/2)\rightarrow5/2^-,5/2$
273.4	1625.4	0.4(1)		$25/2^+,9/2\rightarrow23/2^+,9/2$
273.7	488.3	13.0(6)	0.29(11)	$11/2^-,7/2\rightarrow7/2^-,7/2$
273.9	2282.3	0.2(1)		$25/2^+,17/2\rightarrow23/2^+,17/2$
(274)	(2134)	<0.1		$(23/2^+,19/2)\rightarrow(21/2^+,19/2)$
274.2	1348.8	1.2(6)		$(9/2^-,5/2)\rightarrow5/2^-,5/2$
275.0	$1679.8+\Delta$	2.4(3)	0.26(19)	$(23/2^+,21/2)\rightarrow(21/2^+,21/2)$
279.4	617.5	1.6(2)		$7/2^-,5/2\rightarrow9/2^-,7/2$
280.1	897.3	0.8(1)		$11/2^-,5/2\rightarrow7/2^-,5/2$
283.3	$1688.1+\Delta$	0.9(1)		$(21/2^+,21/2)\rightarrow(21/2^+,21/2)$
287.0	1393.0	7.2(4)	0.00(11)	$27/2^-,25/2\rightarrow25/2^-,25/2$
(287)	$(2258+\Delta)$	<0.1		$(23/2^-,19/2)\rightarrow(21/2^-,19/2)$
294.9	$1974.7+\Delta$	1.4(2)		$(25/2^+,21/2)\rightarrow23/2^+,21/2)$
298.8	1405.0	5.6(5)	$-0.03(11)$	$23/2^+,23/2\rightarrow25/2^-,25/2)$
304.3	519.0	12.5(6)	0.31(16)	$5/2^-,5/2\rightarrow7/2^-,7/2$

TABLE I. *(Continued).*

304.7	985.5	4.9(3)		$13/2^-,1/2 \rightarrow 9/2^-,1/2$
308.6	1713.4	2.5(2)	0.43(25)	$25/2^+,23/2 \rightarrow 23/2^+,23/2$
309.6	1702.0	6.0(4)	0.20(13)	$29/2^-,25/2 \rightarrow 27/2^-,25/2$
313.2	$2287.9 + \Delta$	0.6(1)		$(27/2^+,21/2) \rightarrow (25/2^+,21/2)$
316.5	439.3	12.9(6)	0.22(12)	$15/2^+,9/2 \rightarrow 11/2^+,9/2$
319.8	936.8	2.1(6) [a]		$(7/2^-,3/2) \rightarrow 7/2^-,5/2$
320.2	1256.8	0.5(3) [a]		$(11/2^-,3/2) \rightarrow (7/2^-,3/2)$
326.8	664.8	14.3(7)		$13/2^-,7/2 \rightarrow 9/2^-,7/2$
331.2	2044.7	0.8(1)		$27/2^+,23/2 \rightarrow 25/2^+,23/2$
331.3	2033.9	2.3(3)		$29/2^-,25/2 \rightarrow 27/2^-,25/2$
334.2	1077.0	0.6(1)		$13/2^-,5/2 \rightarrow 9/2^-,5/2$
336.0	3773.9	7(1) [b]		$(43/2^+,43/2) \rightarrow (39/2^-,39/2)$
338.0	338.0	7.9(9) [a]		$9/2^-,7/2 \rightarrow 9/2^+,9/2$
348.4	2897.2	0.6(2)	0.33(25)	$(35/2^-,33/2) \rightarrow (33/2^-,33/2)$
352.5	2397.2	0.7(1)		$29/2^+,23/2 \rightarrow 27/2^+,23/2$
352.8	2386.6	0.8(2)		$31/2^-,25/2 \rightarrow 29/2^-,25/2$
353.3	1196.3	0.8(1)		$15/2^-,1/2 \rightarrow 11/2^-,1/2$
362.9	632.1	10.7(5)	0.26(12)	$17/2^+,9/2 \rightarrow 13/2^+,9/2$
365.5	1675.8	0.6(2) [c]		$(19/2^+,19/2) \rightarrow 17/2^+,17/2$
370.4	3266.4	0.4(1)		$(37/2^-,33/2) \rightarrow (35/2^-,33/2)$
373.2	2770.4	0.1(1)		$31/2^+,23/2 \rightarrow 29/2^+,23/2$
373.5	2760.0	0.2(1)		$33/2^-,25/2 \rightarrow 31/2^-,25/2$
378.2	866.5	8.7(4)	0.31(7)	$15/2^-,7/2 \rightarrow 11/2^-,7/2$
387	1282	0.3(1) [a]		$(15/2^-,5/2) \rightarrow (11/2^-,5/2)$
(391)	(3658)	<0.1		$(39/2^-,33/2) \rightarrow (37/2^-,33/2)$
(392)	(3151)	<0.1		$(37/2^-,25/2) \rightarrow 35/2^-,25/2$
(392)	(3162)	<0.1		$(33/2^+,23/2) \rightarrow 25/2^+,23/2$
396.2	1381.9	2.4(2)	0.31(16)	$17/2^-,1/2 \rightarrow 13/2^-,1/2$
402.8	617.2	3.4(6) [a]		$7/2^-,5/2 \rightarrow 7/2^-,7/2$
410.3	849.6	8.8(4)	0.34(12)	$19/2^+,9/2 \rightarrow 15/2^+,9/2$
422.4	$1827.2 + \Delta$	0.8(2)		$(23/2^-,23/2) \rightarrow (21/2^+,21/2)$
428.4	1093.2	8.7(5)		$17/2^-,7/2 \rightarrow 13/2^-,7/2$
443.2	1754.3	0.4(2)		$21/2^+,17/2 \rightarrow 17/2^+,17/2$
453.9	1086.1	6.0(3)		$21/2^+,9/2 \rightarrow 17/2^+,9/2$
474.1	1856.0	1.0(1)		$21/2^-,1/2 \rightarrow 17/2^-,1/2$
477.9	1344.4	3.7(2)		$19/2^-,7/2 \rightarrow 15/2^-,7/2$
486.4	2008.4	0.3(1)		$23/2^+,17/2 \rightarrow 19/2^+,17/2$
502.3	1352.0	3.0(2)		$23/2^+,9/2 \rightarrow 19/2^+,9/2$
(516)	2548.8	<0.1		$(33/2^-,33/2) \rightarrow 31/2^-,25/2$
525.0	1618.2	1.4(2)		$25/2^+,9/2 \rightarrow 21/2^+,9/2$
531.9	870.1	4.1(9) [a]		$7/2^-,7/2 \rightarrow 9/2^-,7/2)$
539.1	2395.0	0.1(1)		$21/2^-,7/2 \rightarrow 17/2^-,7/2$
539.6	1625.4	1.6(2)		$25/2^-,1/2 \rightarrow 21/2^-,1/2$
549.4	1859.7	1.0(3) [c]		$(21/2^+,19/2) \rightarrow 17/2^+,17/2$
(556)	$(2258+\Delta)$	<0.1		$(23/2^-,19/2) \rightarrow (19/2^-,19/2)$
569.6	$1974.7 + \Delta$	0.5(2)		$(25/2^+,21/2) \rightarrow (21/2^+,21/2)$
571.2	1915.6	0.8(1)		$23/2^-,7/2 \rightarrow 19/2^-,7/2$
591.1	1943.1	0.7(1)		$27/2^+,9/2 \rightarrow 23/2^+,9/2$
597.0	1702.6	5.0(6)		$29/2^-,25/2 \rightarrow 25/2^-,25/2$
607.5	$2287.9 + \Delta$	0.6(2)		$(27/2^+,21/2) \rightarrow (23/2^+,21/2)$
639.4	2044.7	0.2(1)		$27/2^+,23/2 \rightarrow 23/2^+,23/2$
640.4	2033.9	0.5(2)		$31/2^-,25/2 \rightarrow 27/2^-,25/2$
655.9	870.1	5.9(8) [a]		$7/2^-,5/2 \rightarrow 7/2^-,7/2$
678.4	1310.5	0.2(1)		$17/2^+,17/2 \rightarrow 17/2^+,9/2$
683.5	2397.2	0.2(1)		$29/2^+,23/2 \rightarrow 25/2^+,23/2$

TABLE I. *(Continued)*.

683.9	2386.6	0.8(2)		$33/2^-,25/2 \rightarrow 29/2^-,25/2$
718.5	3266.4	0.2(1)		$(37/2^-,33/2) \rightarrow (33/2^-,33/2)$
725.5	2770.4	0.4(1)		$31/2^+,23/2 \rightarrow 27/2^+,23/2$
725.8	2760.0	0.1(1)		$35/2^-,25/2 \rightarrow 31/2^-,25/2$
847.1	2549.0	1.6(2)		$(33/2^-,33/2) \rightarrow 29/2^-,25/2$
860.4	1074.9	10.4(5) [a]		$(5/2^-,5/2) \rightarrow 7/2^-,7/2$
870.1	10(1) [a]	870.1		$7/2^-,7/2 \rightarrow 9/2^+,9/2$
871.1	1310.5	4.6(4)	0.13(17)	$17/2^+,17/2 \rightarrow 15/2^+,9/2$
933.4	1372.8	0.2(1) [c]		$(17/2^+,17/2) \rightarrow 15/2^+,9/2$
1041.0	1310.5	8.6(6)	0.24(14)	$17/2^+,17/2 \rightarrow 13/2^+,9/2$
1052.4	1491.3	0.9(1) [c]		$(17/2^+,17/2) \rightarrow 15/2^+,9/2$
1103.5	1372.8	1.1(2) [c]		$(17/2^+,17/2) \rightarrow 13/2^+,9/2$
1222.0	1491.3	1.7(3) [c]		$(17/2^+,17/2) \rightarrow 13/2^+,9/2$
1351	2457	0.2(1) [d]		$(29/2^-,29/2) \rightarrow 25/2^-,25/2$

[a]Taken from 38 MeV ^{9}Be α-γ-γ, where $I_\gamma[304.3]=88.4$ (*not* normalized to 55 MeV data).

[b]Delayed intensity from gate on γ_{847}, normalized to γ_{287} (μs-chopped 45 MeV ^{7}Li data).

[c]Taken from nanosecond-pulsed 40 MeV ^{9}Be γ-γ data.

[d]Delayed intensity from sum of gates on $\gamma_{171}+\gamma_{336}$, normalized to γ_{348} (μs-chopped 45 MeV ^{7}Li data).

ber in the 38 MeV data obtained here, but was only weakly populated at the two higher bombarding energies.

5. $3/2^-[512]$, $7/2^-[503]$, $1/2^-[521]$, and $5/2^-[523]$ states at 721, 870, 614, and 1075 keV, respectively

Evidence for the population of these states and a few associated rotational levels was found only in the 38 MeV data. They were assigned from comparison with the light-ion transfer data [21–24], and the β^- decay of ^{179}Lu [25]. Most of these states decayed directly or indirectly to the $5/2^-[512]$ state, as shown in Fig. 2.
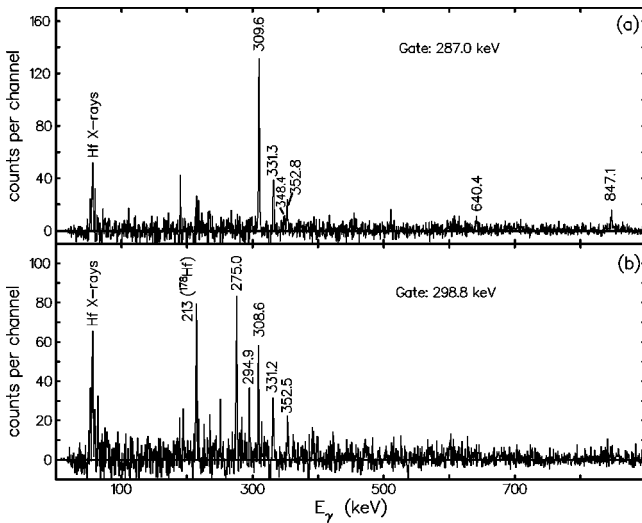
FIG. 5. (a) Coincidence spectrum from a projection made on the 287.0 keV transition in ^{179}Hf, which is assigned as the lowest cascade transition in the rotational band based on the $K^\pi=25/2^-$, $T_{1/2}=25$ day isomer (^{179}Hf^{m2}). (b) Coincidence spectrum made from a projection on the 298.8 keV transition in ^{179}Hf.

B. Three-quasiparticle configurations

1. $K^\pi=25/2^-$, $T_{1/2}=25d$ state at 1106 keV, $^{179}Hf^{m2}$

The only previously known multiquasiparticle state in ^{179}Hf was the $K^\pi=25/2^-$ three-quasiparticle isomer [1,2]. Its metastability ($T_{1/2}=25$ days [3]) makes it a configuration of considerable interest. It is analogous to the $K^\pi=23/2^+$, $T_{1/2}=1.1$ s three-quasiparticle state in ^{177}Hf which arises from coupling the $7/2^-[514]$ ground-state neutron orbital to the $7/2^+[404] \otimes 9/2^-[514]$ excited pair of quasiprotons. In ^{179}Hf, the coupling of the $9/2^+[624]$ ground-state neutron orbital to the same pair of quasiprotons results in the $K^\pi=25/2^-$ configuration. The extracted g_K value agrees well (Table II) with the previously mentioned $\nu 9/2^+ \pi^2[7/2^+, 9/2^-]$ configuration. It is worth noting that there is no ambiguity concerning the purity of the 8^- two-quasiproton component, since the mixing that occurs between the $\nu^2[9/2^+, 7/2^-]$ and $\pi^2[9/2^-, 7/2^+]$ 8^- configurations in the ^{178}Hf core [27] is removed by the addition of the $9/2^+$ quasineutron. This will be discussed in more detail below.

2. $K^\pi=23/2^+$ and $21/2^+$ states at 1405 and $1405+\Delta$ keV, respectively

The two bands that were assigned to ^{179}Hf due to coincidences with the 298.8 keV transition have been placed above ^{179}Hf^{m2}, as is shown in Fig. 3. One is proposed to be based on a $K^\pi=23/2^+$ three-quasiparticle state that arises from the $\nu 7/2^- \pi^2[7/2^+, 9/2^-]$ configuration, where the purity of the $\pi^2 8^-$ component is guaranteed by the presence of the $7/2^-$ quasineutron. The 298.8 keV transition is assigned as the decay from the $K^\pi=23/2^+$ bandhead to the $K^\pi=25/2^-$ state, ^{179}Hf^{m2}. The other band that is coincident with the 298.8 keV transition has been assigned to the $K^\pi=21/2^+$, $\nu 9/2^+ \pi^2[7/2^+, 5/2^+]$ three-quasiparticle state. In both cases

TABLE II. Configurations and g_K factors for single-quasiparticle and multiquasiparticle states in ^{179}Hf.

	Configuration [a]			g_K	
K^π	ν	π	Expt.	Nilsson [d]	Semiempirical [e]
$9/2^+$	$9/2^+[624]$		$-0.22(4)$ [b]	-0.245	
$7/2^-$	$7/2^-[514]$		$0.31(4)$ [b]	0.28	
$5/2^-$	$5/2^-[512]$		$-0.27(12)$ [b]	-0.38	
$1/2^-$	$1/2^-[510]$			-1.79	
$1/2^{-\prime}$	$1/2^-[521]$			0.68	
$17/2^+$			$0.12(4)$ [b]		$0.24(1),(\nu 1/2^- \otimes 8_1^-[^{178}\text{Hf}])$
			$0.48(4)$ [c]		
	$7/2^-,9/2^+,1/2^-$			-0.07	
	$1/2^-$	$7/2^+,9/2^-$		0.84	
	$1/2'^-$	$7/2^+,9/2^-$		0.51	
$21/2^+$	$9/2^+$	$7/2^+,5/2^+$	$0.54(5)$ [c]	0.48	$0.51(8),(\nu 9/2^+ \otimes \pi^2 6^+[^{178}\text{Hf}])$
	$5/2^-$	$7/2^+,9/2^-$		0.67	$0.7(3),\ (\nu 5/2^- \otimes \pi^2 8^-[\text{Nilsson}])$
$23/2^+$	$7/2^-$	$7/2^+,9/2^-$	$0.86(20)$ [c]	0.78	$0.79(10),\ (\nu 7/2^- \otimes \pi^2 8^-[\text{Nilsson}])$
$25/2^-$	$9/2^+$	$7/2^+,9/2^-$	$0.60(7)$ [c]	0.55	$0.56(1),\ (\nu 9/2^+ \otimes \pi^2 8^-[\text{Nilsson}])$
$(33/2^-)$	$1/2^-,7/2^-,9/2^+$	$7/2^+,9/2^-$	$0.46(4)$ [c]	0.45	$0.46(6),\ (\nu 1/2^- \otimes 16^+[^{178}\text{Hf}])$

[a]π:$7/2^+$:$7/2^+[404]$; $9/2^-$:$9/2^-[514]$; $5/2^+$:$5/2^+[402]$. ν: as shown.

[b]$(g_K-g_R)/Q_0$ negative, $Q_0=6.95(6)e$ b, $g_R=0.22(3)$ (one-quasiparticle states), and $g_R=0.3$ ($17/2^+$ state).

[c]$(g_K-g_R)/Q_0$ positive, $Q_0=6.95(6)e$ b, $g_R=0.34(5)(25/2^-$, $23/2^+$, and $21/2^+$ states), and $g_R=0.3$ ($17/2^+$ and $(33/2^-)$ states).

[d]Nilsson wave functions, $g_s=0.7g_{free}$, deformations of $(\varepsilon_2,\ \varepsilon_4)=(0.254,0.053)$.

[e]Combination of present single-quasineutron g_K values with multiquasiparticle components from ^{178}Hf [14] where available, otherwise Nilsson value used for (pure) $\pi^2 8^-$ ($g_K=1$).

the mean g_K values extracted from the in-band branching ratios are in reasonable agreement with the Nilsson and semiempirical predictions. A spectrum of the intermediate time between the 298.8 keV transition and the lowest $23/2^+$ band member (308.6 keV) is consistent with a half-life of 4(1) ns, as is shown in Fig. 6(b). It is proposed that the $21/2^+$ band head decays to the $23/2^+$ state, since if it fell below the latter, it would have to decay to the $25/2^-$ isomer via an $M2$ transition. A lifetime in the region of microseconds would then be expected, whereas a half-life of 14(2) ns was derived from a projection of the time difference between the 298.8 keV transition and the 275.0 keV $21/2^+$ band member, as is shown in Fig. 6(c). There was no evidence for a $21/2^+ \rightarrow 23/2^+$ γ-ray transition, presumably because it has low energy and is heavily converted. This concurs with our multiquasiparticle calculations, which predict that the $23/2^+$ and $21/2^+$ states should lie close in excitation energy (Table III).

Two other γ-ray transitions were found to be in coincidence with the 298.8 keV transition, and they both showed time correlations consistent with their placement above the $21/2^+$ state. The 283.3 keV transition may decay from a $K^\pi=19/2^-$ three-quasiparticle $\nu 7/2^- \pi^2[5/2^+,7/2^+]$ configuration. No branching ratio information could be extracted from the band built on this state, since it was possible to identify only the first cascade transition. The 422.4 keV transition may decay from a second $K^\pi=21/2^+$ state that is expected from the $\nu 5/2^- \pi^2[7/2^+,9/2^-]$ configuration.
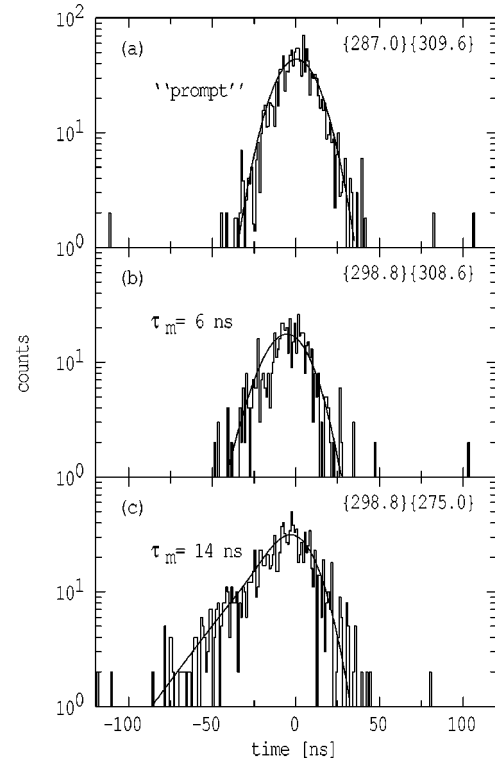
FIG. 6. Intermediate time spectra between (a) the 287.0 and the 309.6 keV transitions, (b) the 298.8 keV and the 308.6 transitions, and (c) the 298.8 keV transition and the 275.0 keV transitions, in ^{179}Hf.

TABLE III. Calculated and observed excitation energies for multiquasiparticle states in ^{179}Hf.

	Configuration [a]			Energy (keV)		
K^π	ν	π	E_{qp}	E_{resid}	E_{calc}	E_{expt}
$9/2^+$	$9/2^+$		0	0	0	0
$7/2^-$	$7/2^-$		176	0	176	214
$5/2^-$	$5/2^-$		394	0	394	519
$1/2^-$	$1/2^-$		528	0	528	375
$1/2^-$	$1/2^{-\prime}$		565	0	634	614
$3/2^-$	$3/2^-$		659	0	659	720
$7/2^-$	$7/2^{-\prime}$		802	0	802	870
$17/2^+$	$7/2^-,9/2^+,1/2^-$		1677	−131	1546	1310
$17/2^+$	$1/2^-$	$7/2^+,9/2^-$	1782	−143	1639	(1372)
$17/2^+$	$1/2^{-\prime}$	$7/2^+,9/2^-$	1818	−85	1733	(1491)
$19/2^-$	$7/2^-$	$7/2^+,5/2^+$	1647	−223	1424	$(1688+\Delta)$
$19/2^+$	$7/2^-,9/2^+,3/2^-$		1805	−55	1750	
$19/2^+$	$3/2^-$	$7/2^+,9/2^-$	1912	−98	1814	
$21/2^+$	$9/2^+$	$7/2^+,5/2^+$	1471	−193	1278	$1405+\Delta$
$21/2^+$	$5/2^-$	$7/2^+,9/2^-$	1647	−151	1495	$(1827+\Delta)$
$23/2^+$	$7/2^-$	$7/2^+,9/2^-$	1429	−200	1229	1405
$25/2^-$	$9/2^+$	$7/2^+,9/2^-$	1252	−129	1123	1106
$29/2^-$	$3/2^-,9/2^+,1/2^{-\prime}$	$7/2^+,9/2^-$	3450	−190	3260	(2457)
$29/2^+$	$7/2^-,9/2^+,1/2^-$	$7/2^+,5/2^+$	3148	−397	2751	
$31/2^+$	$7/2^-,9/2^+,3/2^-$	$7/2^+,5/2^+$	3276	−290	2996	
$31/2^-$	$5/2^-,9/2^+,1/2^-$	$7/2^+,9/2^-$	3150	+306	3456	
$33/2^-$	$7/2^-,9/2^+,1/2^-$	$7/2^+,9/2^-$	2930	−359	2571	2549
$33/2^+$	$7/2^-,9/2^+,7/2^{-\prime}$	$7/2^+,5/2^+$	3635	−313	3322	
$35/2^-$	$7/2^-,9/2^+,3/2^-$	$7/2^+,9/2^-$	3058	−237	2821	
$35/2^+$	$7/2^-,9/2^+,7/2^{-\prime}$	$7/2^+,5/2^+$	3419	−313	3106	
$35/2^+$	$7/2^-,5/2^-,7/2^{-\prime}$	$7/2^+,9/2^-$	3605	−473	3132	
$39/2^-$	$7/2^-,9/2^+,7/2^{-\prime}$	$7/2^+,9/2^-$	3201	−269	2932	3437
					3347 [b]	
$43/2^+$	$7/2^-,9/2^+,11/2^+$	$7/2^+,9/2^-$	4315	−272	4043	3774
$47/2^-$	$7/2^-,9/2^+,7/2^{-\prime},3/2^-,5/2^-$	$7/2^+,9/2^-$	5151	−517	4634	

[a]Single-quasiparticle orbitals labeled with asymptotic Nilsson quantum numbers; ν:$9/2^+$:$9/2^+$[624]; $7/2^-$:$7/2^-$[514]; $5/2^-$:$5/2^-$[512]; $1/2^-$:$1/2^-$[510]; $1/2^{-\prime}$:$1/2^-$[521]; $3/2^-$:$3/2^-$[512]; $7/2^{-\prime}$:$7/2^-$[503]; $11/2^+$:$11/2^+$[615]; π:$7/2^+$:$7/2^+$[404]; $9/2^-$:$9/2^-$[514]; $5/2^+$:$5/2^+$[402].
[b]Empirical estimate, $E_x(39/2^-)=E_x(16^+[^{178}\text{Hf}])+E_x(\nu 7/2^-[503])+E_{resid}(=30 \text{ keV})$.

3. $K^\pi=17/2^+$ state at 1311 keV

The only three-quasiparticle band that could be connected directly to known states in ^{179}Hf decayed to the $13/2^+$, $15/2^+$, and $17/2^+$ members of the $9/2^+$ ground-state band, consistent with an assignment of $K^\pi=17/2^+$ to the bandhead. Our multiquasiparticle calculations indicate three possible $K^\pi=17/2^+$ configurations that should lie within ~ 200 keV of each other (see Table III). The lowest of these is the $\nu^3[1/2^-[510],7/2^-,9/2^+]$ configuration, while the next two, in increasing order of energy, are the $\nu 1/2^-[510]\pi^2[7/2^+,9/2^-]$ and $\nu 1/2^-[521]\pi^2[7/2^+,9/2^-]$ configurations. Hence, the calculations suggest that the two lowest states can be considered as coupling of the $\nu 1/2^-[510]$ orbital (which is 239 keV lower in excitation

than the $\nu 1/2^-[521]$ orbital) to the 8^- two-quasiproton and two-quasineutron components in the ^{178}Hf core. These two-quasiparticle $K^\pi=8^-$ core-states are, as noted earlier, known to be mixed, which suggests that the 8^- component in each of the $17/2^+$ configurations in ^{179}Hf will probably not be pure. In this case the g_K value for the $17/2^+$ band will deviate from that expected for the unmixed configuration. Unfortunately, the sign of $(g_K-g_R)/Q_0$ could not be determined, due to the weakness of the cascade transitions in the particle-γ data. If the negative sign is taken, then the low g_K value obtained (Table II) suggests that the dominant component in the configuration is ν^3. If the positive sign is taken, then the g_K value is in accordance with the pure $\nu 1/2^-[521]\pi^2 8^-$ configuration, but considerations of the relative excitation

energies of the possible $17/2^+$ configurations (Table III) make this a doubtful scenario. *A priori* it might be expected that the g_K value obtained from combining the lower of the mixed 8^- states observed in ^{178}Hf with the $1/2^-[510]$ orbital would agree with experiment, but this is not the case (Table II). The problem can be inverted by using additivity to obtain the g_K value for the 8^- component from the experimental g_K value for the $17/2^+$ band, if the Nilsson g_K value for the $1/2^-[510]$ neutron orbital is assumed. The result is $g_K = 0.62(2)$ for the 8^- component, consistent with a $\nu^2[36\%]\pi^2[64\%]$ mixture, which suggests that the relative energies of the unmixed π^2 and $\nu^2 8^-$ components in ^{179}Hf have shifted as the neutron Fermi level moves higher. This suggestion is consistent with the fact that the $K^\pi = 8^-$ isomeric states in ^{180}Hf and ^{182}Hf have essentially pure π^2 character [28,29].

Candidates for the related $K^\pi = 17/2^+$ state, which would arise from the complementary $8^- \nu^2[64\%]\pi^2[36\%]$ mixed component coupled with the $1/2^-[510]$ neutron, are limited to a few weakly populated states that are shown in Fig. 2. These states were only observed in the 38 MeV α-γ-γ and the 40 MeV archived data. Two of them decay both to the $15/2^+$ and $13/2^+$ members of the ground-state band, which is consistent with assignments of $K^\pi = 17/2^+$. This suggests, in accordance with the multiquasiparticle calculations, that there might be two higher $K^\pi = 17/2^+$ configurations. No associated rotational transitions could be found in either case, but there are also three other states that decay directly to the lowest $K^\pi = 17/2^+$ state. These states may be unrelated, but they could be rotational levels associated with one or both of the higher $17/2^+$ configurations.

C. Five-quasiparticle configurations

1. $K^\pi = (33/2^-)$ state at 2549 keV

The 847.1 keV transition to the $29/2^-$ rotational level associated with the $K^\pi = 25/2^-$ isomer was assumed to have stretched $E2$ character, and hence that it decayed from a $K^\pi = (33/2^-)$ state. This is consistent with the evidence for a weak 516 keV transition to the $31/2^-$ band member and the lack of a transition to the $27/2^-$ rotational state. The lowest two cascade transitions could be confidently assigned to the band based on the $K^\pi = (33/2^-)$ state, with a weak crossover transition that was more clearly observed in the measurement made with the ^{7}Li chopped beam. Our multiquasiparticle calculations predict (Table III) that a five-quasiparticle, $K^\pi = 33/2^-$ state, which arises from the $\nu^3[7/2^-,9/2^+,1/2^-]\pi^2[7/2^+,9/2^-]$ configuration, should lie close to the observed excitation energy. The branching ratio obtained from μs-chopped ^{7}Li data was consistent with a g_K value that agreed with this configuration assignment. A half-life of 30(10) ns was obtained from a projection of the intermediate coincidence time between transitions above and below the $K^\pi = (33/2^-)$ state.

2. $K^\pi = (39/2^-)$ and $(43/2^+)$ states at 3438 and 3374 keV, respectively

Two higher-lying five-quasiparticle states were found when a spectrum was projected in coincidence with the
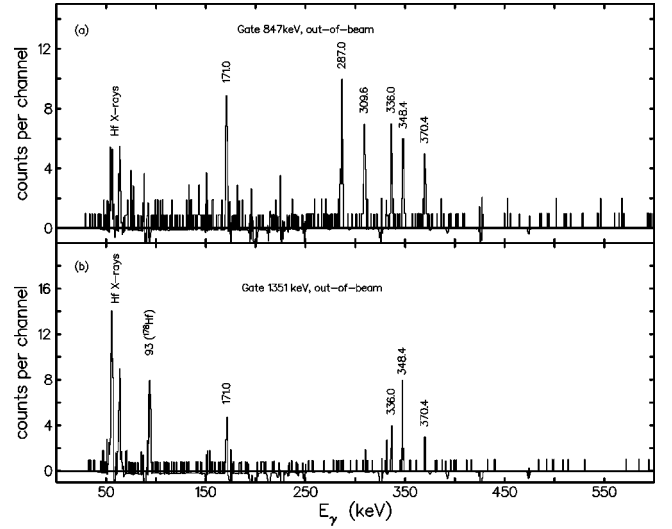
FIG. 7. Coincidence spectra gated by (a) the 847.1 keV transition and (b) the 1351 keV transition, obtained from the out-of-beam (45 MeV^{7}Li) data in the time region 0–80 μs. The relatively strong Hf x rays arise in spectrum (b) from electron conversion of the 93 keV $2^+ \to 0^+$ transition in ^{178}Hf, which is in delayed coincidence with the 1351 keV line via β^+/EC decay of ^{178}Ta.

847.1 keV transition from the microsecond-chopped ^{7}Li-induced data in the out-of-beam time region. This spectrum, with a time condition optimized such that the pair of coincident γ rays were recorded within 80 μs of the beam burst, is shown in Fig. 7(a). In addition to the two lowest members of both the $25/2^-$ and $33/2^-$ bands, peaks at $E_\gamma = 171$ and 336 keV can be seen. These transitions were found to be mutually coincident, which suggests that they decay sequentially from a long-lived state into the $37/2^-$ member of the $33/2^-$ band. A fit to the time spectrum projected on the 847.1 keV transition is consistent with a half-life of 15(5) μs of the isomeric state, as is shown in Fig. 8. The ordering of the two transitions was fixed by the observation that the 171 keV transition decayed with a half-life of 12(6) ns when a projection of the intermediate coincidence time was made between the 336 keV transition and the $K^\pi = (33/2^-)$ band members. Delayed intensity balances suggest that the 171 keV transition has a total conversion coefficient of $\alpha_{tot} = 0.7(3)$, which is consistent with a mixed $M1/E2$ character. Similarly, $\alpha_{tot} = 0.5(3)$ was found for the 336 keV transition, which is consistent with an $M2$ assignment. This suggests that the 171 keV transition probably decays from a $K^\pi = 39/2^-$ five-quasiparticle state which arises from the $\nu^3[7/2^-,9/2^+,7/2^-]\pi^2[7/2^+,9/2^-]$ configuration. The $M2$ assignment to the 336 keV transition suggests that it deexcites a $K^\pi = 43/2^+$ state which most likely arises from the $\nu^3[7/2^-,9/2^+,11/2^+]\pi^2[7/2^+,9/2^-]$ five-quasiparticle configuration.

3. $K^\pi = (29/2^-)$ state at 2457 keV

When out-of-beam coincidence projections were made on the transitions that constitute the decay path from the $K^\pi = 43/2^+$ state to the $K^\pi = 33/2^-$ state, a 1351 keV transition
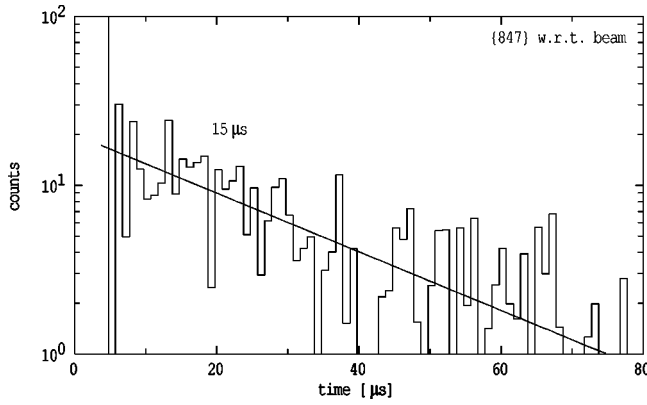
FIG. 8. Decay spectrum that illustrates the lifetime of the $K^\pi = (43/2^+)$ state at 3774 keV. The spectrum corresponds to the time at which the 847 keV transition was detected relative to the beam burst in the microsecond-chopped ^{7}Li data. The line corresponds to a half-life of 15 μs.

FIG. 9. Plot of excitation versus spin for calculated (large open symbols) multiquasiparticle states and experiment (large solid symbols) for ^{179}Hf. Rotational states associated with a particular multiquasiparticle configuration are shown as the small solid symbols, connected by a solid line. The band based on the $K^\pi = 9/2^+$ ground state is shown for comparison, while the ''*'' depicts the lowest seven-quasparticle state predicted by the calculations ($K^\pi = 47/2^-$).

was common to all spectra. This is illustrated in Fig. 7(b) in which a spectrum of transitions in the delayed-time region, but in prompt coincidence with the 1351 keV line, is shown. The absence of coincidences with the 287.0 and 309.6 keV $K^\pi = 25/2^-$ band members suggests that the 1351 keV transition decays directly to ^{179}Hf^{m2} from a state at 2457 keV, as is shown in Fig. 3. The placement of the 1351 keV transition was confirmed by the observation of prompt coincidences between it and the 348.4, 370.4, and 171.0 keV transitions in the particle-γ-γ data obtained with the ^{7}Li beam. These observations clearly suggest that there is a decay branch from the $K^\pi = 33/2^-$ state at 2548.8 keV to the state at 2457 keV, with a transition energy of 91 keV. The line close to this energy in Fig. 7(b) is in fact the 93 keV $2^+ \to 0^+$ transition in ^{178}Hf, which is in coincidence with a 1351 keV transition that deexcites a $K^\pi = 0^+$ vibrational state populated in the $T_{1/2} = 9.3$ min β^+/EC decay of ^{178}Ta [30,31]. Since the 91 keV γ-ray transition had no measurable intensity, an $E1$ assignment could be excluded on the basis of the limit on the implied conversion, which rules out an assignment of $J^\pi = 31/2^+$ to the state at 2457 keV. An $M2$ assignment to the 91 keV transition can be ruled out, since the corresponding partial γ-ray half-life would be ~ 1 ms. The most likely assignment to the 91 keV transition is either $M1$ or $E2$, so that the state at 2457 keV has either $J^\pi = 31/2^-$ or $29/2^-$, respectively. The $J^\pi = 31/2^-$ assignment can be rejected, since the absence of a measurable lifetime for the 1351 keV transition is inconsistent with an $M3$ character. Thus, the state at 2457 keV is assigned $J^\pi = 29/2^-$, which implies $E2$ character for both the 91 and 1351 keV transitions. Neither transition is K forbidden, which allows the 91 keV $E2$ to compete with the twice-forbidden 847.1 keV $E2$ in the deexcitation of the $K^\pi = 33/2^-$ state. If the level at 2457 keV is an intrinsic state, it would have $J^\pi = K^\pi = 29/2^-$. The lowest $29/2^-$ state predicted by the multiquasiparticle calculations (Table III) arises from the $\nu^3[3/2^-, 1/2^{-\prime}, 9/2^+]\pi^2[7/2^+, 9/2^-]$ configuration, which falls considerably higher at ~ 3300 keV, as will be discussed below.

V. DISCUSSION

A. Comparison with blocked multiquasiparticle calculations

It is instructive to plot the level structure of ^{179}Hf in a conventional excitation energy versus spin diagram, and then compare with predictions of multiquasiparticle calculations. This is a useful means with which to track the evolution of the yrast (and near-yrast) line in order to identify favored configurations. The recipe for these types of calculation has been outlined in a number of previous publications [32,13]. In the present case, the single-quasiproton and single-quasineutron energies from a Nilsson model calculation were adjusted to approximate the experimental states in ^{179}Ta and ^{179}Hf, respectively. The pairing strengths were fixed at $G_\pi = 19.2/A$ MeV and $G_\nu = 18.0/A$ MeV, with blocking of specific orbitals in multiquasiparticle configurations accounted for within the Lipkin-Nogami formalism. Configuration-dependent residual interactions were evaluated with the method of Jain *et al.* [33], in which the contribution of each two-quasiparticle component was summed, with the Gallagher-Moszkowski splittings taken from experiment. The comparison is presented in the form of a plot (Fig. 9) and in Table III. The agreement of the calculations and experiment to within ~ 20 keV for the $K^\pi = 25/2^-$ and the $K^\pi = (33/2^-)$ states is presumably fortuitous. The comparison for other states suggests that an agreement to within ~ 200 keV is a more realistic expectation.

The calculations predict that the $K^\pi = 39/2^-$ state should be low lying, and, on the basis of the K-selection rule, would be expected to decay to rotational states based on the $K^\pi = 33/2^-$ configuration. This is consistent with the assignment of $K^\pi = 39/2^-$ to the state at 3438 keV, though the calculations predict it to be rather more favored, with an excitation energy of 2.9 MeV. If, however, the excitation energy of the $39/2^-$ configuration is estimated by simply adding the energy of the $7/2^-[503]$ orbital to that of the observed 16^+ state in the ^{178}Hf core, a value of 3.3 MeV results.

It is worth noting that the $39/2^-$ configuration in ^{179}Hf may be also be regarded as a $5/2^+[402]$ proton removed from a 22^- six-quasiparticle configuration calculated to occur in the isotone ^{180}Ta [13]. The 22^- state was predicted to fall so low in energy in ^{180}Ta that it could have been metastable. This state was not observed, presumably because it was at the limit of the maximum angular momentum with which ^{180}Ta was populated, although in retrospect the present results suggest that both it and the $39/2^-$ state in ^{179}Hf were predicted too low in energy.

The calculations also predict that the $K^\pi = 43/2^+$, $\nu^3[7/2^-,9/2^+,11/2^+]\pi^2[7/2^+,9/2^-]$ configuration should fall at an excitation energy of 4.0 MeV (Table III). This is in acceptable accordance with the experimental value of 3.77 MeV. The $K^\pi = 43/2^+$ state can also be related to a favored, but presently inaccessible, $K^\pi = 24^+$ six-quasiparticle state predicted to occur in ^{180}Ta [13] by the removal of the $5/2^+[402]$ proton. The $43/2^+$ configuration may be regarded as coupling the 16^+ core state to the $11/2^+[615]$ orbital, but the latter has not been observed experimentally in ^{179}Hf. This orbital has been invoked, however, as a component in a $K^\pi = 10^+$ two-quasiparticle isomeric state in ^{180}Hf [28]. It is also probably implicated in the $K^\pi = 18^{(+)}$ four-quasiparticle $\nu^3[9/2^+,7/2^-,11/2^+]\pi 9/2^-$ state in ^{180}Ta.

The interpretation of the $K^\pi = (29/2^-)$ state at 2457 keV as the lowest five-quasiparticle configuration in ^{179}Hf is problematic, since the multiquasiparticle calculations predict (Table III) it to fall ~ 700 keV higher in excitation energy than the $K^\pi = 33/2^-$ state. Indeed, a number of other five-quasiparticle configurations with the same or higher spin are predicted to be more favored. An alternative explanation could be that the $29/2^-$ state arises from a $K^\pi = 2^+$ phonon coupled to ^{179}Hf^{m2}. Recent calculations of vibrational states built on ^{179}Hf^{m2} have been carried out [34], and these predict that the lowest mode should give rise to a $K^\pi = 29/2^-$ state at an excitation energy of 2.2 MeV. The calculations have an expected accuracy of ± 0.2 MeV [34], so the predicted excitation energy is consistent with the present experimental value of 2.457 MeV.

A final point worth noting is the prediction of a favored seven-quasiparticle state with $K^\pi = 47/2^-$ at 4.6 MeV, which is lowered by an attractive residual interaction of ~ 0.5 MeV. This state could be yrast, and would be expected to decay to members of the $K^\pi = 43/2^+$ band.

B. Gyromagnetic ratios

1. Intrinsic g_K factors

The g_K factors extracted for each band are shown in Table II, where they are compared with values calculated from the Nilsson model and with semiempirical estimates. The agreement with the Nilsson model is generally good enough to confirm the configuration assignments, in the sense that all other plausible alternatives could be rejected. A slight improvement is achieved when empirical values are used.

The situation regarding the band assigned to the $K^\pi = 17/2^+$ three-quasiparticle configuration is not clear, as was discussed earlier. The interpretation depends largely on the degree of mixing between the two 8^- components which affects the composition of the $17/2^+$ configuration. In contrast the 8^- component in the $\nu 9/2^+ \otimes \pi^2 8^-$ configuration for the $K^\pi = 25/2^-$ isomer *has* to have pure two-quasiproton character. This is because the 8^- two-quasineutron state arises from coupling the $9/2^+[624]$ and $7/2^-[514]$ orbitals. The occupancy of the $9/2^+[624]$ orbital in the $25/2^-$ configuration blocks the two-quasineutron amplitude in the 8^- component, so it has to have pure two-quasiproton character. This can be demonstrated if the empirical g_K value for the $\nu 9/2^+$ state is placed in the additivity relation

$$Kg_K = \sum \Omega_i g_i$$

in order to extract the g_K value for the 8^- component of the $25/2^-$ state. This gives $g_K(8^-) = 1.06(11)$, which is indeed consistent with the Nilsson model value for a pure two-quasiproton state [35]. For comparison, a value of $g_K(8^-) = 1.08(5)$ was derived from the magnetic moment of ^{179}Hf^{m2} [4]. Since the latter result was consistent with a value greater than unity, it was taken as evidence for an anomalous contribution to the proton magnetic moment from meson-exchange effects [36]. Unfortunately the error on the present value is too large to enable confirmation of this result.

2. Collective g factors for the ground state and ^{179}Hf^{m2}

The parameter g_R represents the effective g factor that arises from rotational motion in a $K = 0$ band so that [37]

$$\mu = g_R I.$$

It characterizes the fractional contribution of the protons to the nuclear magnetic moment, which suggests it can be written as

$$g_R = \frac{Z\mathcal{J}_\pi}{Z\mathcal{J}_\pi + N\mathcal{J}_\nu}, \quad (1)$$

where $\mathcal{J}_\pi$ ($\mathcal{J}_\nu$) corresponds to the proton (neutron) moment of inertia. An increase in $\mathcal{J}_\pi$ will therefore lead to a larger value of g_R, while the opposite is true if $\mathcal{J}_\nu$ increases. Superfluid pairing correlations tend to reduce $\mathcal{J}$, so that a reduction in pairing strength, through, for example, blocking due to quasiparticle excitations, is expected to increase the moment of inertia.

For bands with $K > 1/2$, the intrinsic motion contributes to the magnetic moment, so that

$$\mu = g_R I + (g_K - g_R)\frac{K^2}{(I+1)}.$$

The quantity $(g_K - g_R)$ can be evaluated from in-band branching ratios, provided the intrinsic quadrupole moment is known. In the case of ^{179}Hf, the magnetic moments of the $9/2^+$ state [38] and the $25/2^-$ isomer [4] have been measured, and hence can be combined with the values of $(g_K - g_R)$ to find g_R for these two configurations. A value of $g_R = 0.221(25)$ was found for the $\nu 9/2^+$ band, which can be compared with $g_R = 0.230(19)$ for the $\nu 7/2^-$ ground-state band in ^{177}Hf [39]. This rules out the large decrease in the ground-state g_R from ^{177}Hf ($g_R = 0.24$–0.28) to ^{179}Hf($g_R = 0.12$–0.14) that was predicted by cranking-model calculations [40]. The value extracted for g_R in the three-quasiparticle $25/2^-$ band was considerably higher, $0.34(5)$. In the $\nu \otimes \pi^2 K^\pi = 25/2^-$ configuration, our blocked Lipkin-Nogami pairing calculations suggest that the proton pairing in the $25/2^-$ configuration is reduced to $\sim 70\%$ of the ground-state value. Though recent results for ^{179}W [41] and ^{178}W [42] suggest that the Lipkin-Nogami method probably overestimates pairing, when this value is inserted in the Migdal two-fluid formula and the resultant moment of inertia is used in Eq. (1), an increase of $\delta g_R \simeq +0.07$ is predicted relative to that of the ground state. This is consistent with the experimental increase of $\delta g_R \simeq +0.12(6)$.

C. Alignments

1. General comments

Net alignments have been extracted for the rotational bands in ^{179}Hf, and are plotted relative to a common Harris reference rotor in Fig. 10(a). A few points are worth noting. The alignments of the one-quasineutron $9/2^+$ band begin to oscillate beyond a rotational frequency of $\hbar\omega \simeq 0.2$ MeV, indicative of Coriolis-induced K mixing with the other members of the $i_{13/2}$ multiplet. The magnitude of the oscillations is considerably smaller than that seen in the analogous bands in either the isotone ^{181}W or in ^{177}Hf. This suggests that the K mixing in the $\nu 9/2^+$ band in ^{179}Hf is weaker than in the other two nuclei, which is consistent with the extracted g_K values as discussed earlier, since, unlike ^{179}Hf, they deviate considerably from the Nilsson model estimates.

Of the three-quasiparticle bands, the one based on the $K^\pi = 25/2^-$ state has the largest alignment, consistent with the presence of an $i_{13/2}$ neutron. The same neutron orbital is occupied in the $K^\pi = 21/2^+$ configuration, but the net alignment is lower, probably due to the smaller contribution of the $\pi^2 6^+$ component compared to that of the $\pi^2 8^-$ component in the $K^\pi = 25/2^-$ configuration. The alignments of the $K^\pi = 23/2^+$, $K^\pi = 17/2^+$, and $K^\pi = 25/2^- \nu\pi^2$ bands, relative to one another, are approximately consistent with the relative values of their respective single-quasineutron components, namely, the $7/2^-$, $1/2^-$, and $9/2^+$ one-quasineutron bands.

The $K^\pi = 33/2^-$ five-quasiparticle band has the highest alignment of all the rotational structures observed thus far in ^{179}Hf. This is to be expected, due to the presence of an extra two unpaired neutrons compared to, for example, the K^π
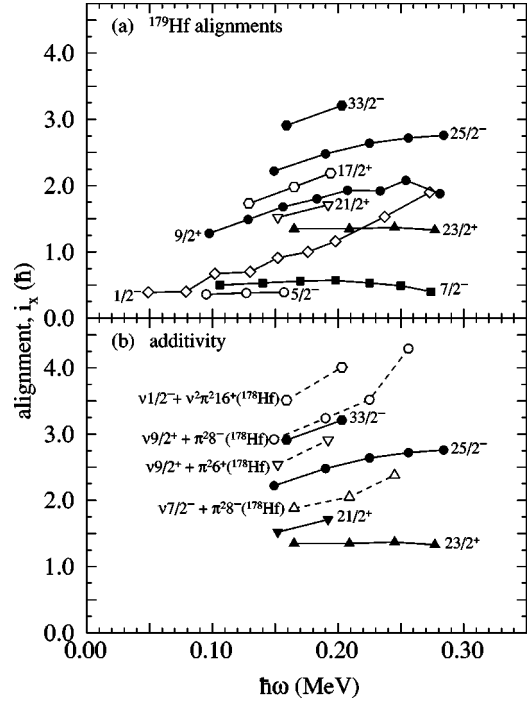
FIG. 10. (a) Aligned angular momenta for rotational bands in ^{179}Hf, calculated with constant K values taken from the respective bandheads. The Harris reference parameters used were $\mathcal{J}_0 = 31.8\hbar^2/$MeV and $\mathcal{J}_1 = 70\hbar^4/$MeV^3. (b) Additivity comparison between alignments for some multiquasiparticle bands in ^{179}Hf (solid symbols, solid lines) with ''equivalent'' configurations (open symbols, dashed lines) constructed from core components in ^{178}Hf [14] and single-quasineutron bands in ^{179}Hf.

$= 25/2^-$ band which has the largest alignment of the three-quasiparticle configurations. In ^{177}Hf, however, the alignment of the $K^\pi = 25/2^-$ three-quasiparticle band is *higher* than that of the $K^\pi = 37/2^-$ five-quasiparticle band [17], and there are many other cases where this effect is seen, as discussed in Ref. [43]. This seemingly anomalous behavior is proposed to be due to reduced pairing, which is expected to increase the moment of inertia of the collective core, while reducing the alignment contributed by the component quasiparticles. An apparent increase in alignment will result *if the collective moment of inertia increases and the Harris reference used is that which is more appropriate for the maximally paired, low-seniority states. If the reduction in quasiparticle alignment is greater than this artificial increase, however, then a lower net alignment can result for a configuration of higher seniority, when compared to that of related configuration of lower seniority. Clearly this is a configuration-dependent effect, since the $K^\pi = 39/2^+$ five-quasiparticle band in ^{177}Hf, which contains two $i_{13/2}$ neutrons, has a larger alignment than that of the $K^\pi = 25/2^-$ band in this nucleus. It would be of interest to find the rotational band based on the $K^\pi = 43/2^+$ state in ^{179}Hf, since it too contains two $i_{13/2}$ neutrons.

2. Additivity

The alignments for some of the bands based on multiquasiparticle configurations in ^{179}Hf can, in principle, be con-

TABLE IV. Reduced hindrances for K-forbidden transitions in ^{179}Hf.

K^π	$T_{1/2}$ (ns)	E_γ (keV)	I_γ	$L\lambda$	α_{tot}	ΔK	ν	$T_{1/2}^\gamma$ (ns)	$T_{1/2}^{W.u.}$ (s)	f_ν
$17/2^+$	3(1)	1041	8.6(6)	$E2$	0.004	4	2	5(2)	7.7×10^{-12}	25(5)
		871	4.6(4)	$M1$	0.012	4	3	9(3)	3.3×10^{-14}	65(7)
		678	0.4(2)	$(M1)$	0.023	4	4	103(34)	7.1×10^{-14}	35(3)
$33/2^-$	30(10)	847	1.6(2)	$E2$	0.006	4	2	30(10)	2.15×10^{-11}	37(6)
$39/2^-$	12(6)	171	5(1)	$M1$	0.9	3	2	23(12)	4.4×10^{-12}	72(18)

structed from two- and four-quasiparticle bands in ^{178}Hf [14] combined with the relevant single-quasineutron band in ^{179}Hf. Since the $K^\pi=25/2^-$ and $23/2^+$ configurations contain a pure $\pi^2[8^-]$ component, it was necessary to calculate the alignment for the uncoupled $\pi^2[8^-]$ states by removing the mixing with the $\nu^2[8^-]$ states in the ^{178}Hf core. The results of the "additivity" are shown in Fig. 10(b) for the $K^\pi=21/2^+$, $23/2^+$, $25/2^-$, and $33/2^-$ configurations in ^{179}Hf. In all cases, the constructed alignments are greater than those obtained for the configuration itself. This failure of additivity in the $\nu\pi^2$ configurations suggests that the alignment of the "bare" single-quasineutron orbitals is reduced by the presence of the pair of decoupled quasiprotons. The addition of the $1/2^-[510]$ neutron to the $\nu^2\pi^2K^\pi=16^+$ core state would be expected to reduce the neutron pairing by blocking, and hence lessen the alignment of the quasineutrons in the resultant $K^\pi=33/2^-$ configuration, a feature not taken into account.

D. K-hindered transitions from multiquasiparticle states

The degree of K forbiddenness of a transition of multipolarity λ between two states that differ in K by ΔK is defined as $\nu=\Delta K-\lambda$. If $\nu>0$, then the transition is "K forbidden," but in practice admixtures of other K values into the wave functions of one or other or both of the states lead to hindered decays. These hindered decays still obey the K-selection rule in the sense that they proceed via the minimum change in K. A useful measure of the extent to which the K-selection rule is obeyed is the hindrance per degree of K forbiddenness, f_ν, or reduced hindrance for short. It is defined as

$$f_\nu=\left(\frac{T^\gamma}{T^W}\right)^{1/\nu},$$

where T^γ is the partial γ-ray lifetime, and T^W is the Weisskopf single-particle estimate.

The details of K-hindered transitions in ^{179}Hf are listed in Table IV, where the f_ν values are listed for decays from the $K^\pi=17/2^+$, $33/2^+$, and $39/2^-$ multiquasiparticle states. In general the reduced hindrances are in the range 25–75, but have large errors of the order of $\sim$10–25 %, which arise from the uncertainties in the lifetimes of the states. Even so, these f_ν values indicate that the transitions from the intrinsic multiquasiparticle states to rotational levels based on the lower-lying configuration proceed in accordance with the K-selection rule.

It is worth noting that the reduced hindrance obtained for the 171 keV $\nu=2$ decay from the $K^\pi=39/2^-$ state ($f_\nu\simeq70$) offers an explanation as to why the 541 keV $E2$, $\nu=1$ decay from the same state was not observed. If the same reduced hindrance is assumed for the 541 keV transition, it would constitute less than a 1% branch of the decay from the $K^\pi=39/2^-$ state.

VI. SUMMARY

Time-correlated particle-γ-γ spectroscopy has been employed to study the level structure at moderate spins of the stable nucleus ^{179}Hf. These measurements have enabled states above the $T_{1/2}=25$ day, $K^\pi=25/2^-$ isomer to be studied for the first time, and allowed the rotational band based on the isomer to be established. The g_K value derived from the in-band branching ratios is consistent with the previously suggested $\nu9/2^+\otimes\pi^2[7/2^+,9/2^-]$ configuration. The collective g factor (g_R) derived for this state was 0.34(5), which is considerably higher than the value of 0.221(25) for the $9/2^+$ ground state.

A number of five-quasiparticle states were found above the 25 day isomer. These included a $K^\pi=33/2^-$ configuration for which an associated rotational band was found. Delayed feeding was observed into the $37/2^-$ level of this band. This came from the decay of a $K^\pi=(43/2^+)$, $T_{1/2}=15(5)$ μs state, which deexcited via a $K^\pi=(39/2^-)$ state into the $37/2^-$ rotational band member.

Multiquasiparticle calculations, which reproduce the excitation energies of the three- and five-quasiparticle states to within $\sim$200 keV, predict that the lowest seven-quasiparticle state will arise from a $K^\pi=47/2^-$ configuration. It would be expected to decay to members of the band based on the $K^\pi=43/2^+$ state, but confirmation of this prediction would require ^{179}Hf to be populated at higher angular momentum than was possible with the incomplete fusion reactions employed here.

[1] H. Hübel, R. A. Naumann, M. L. Anderson, J. S. Larsen, O. B. Nielsen, and N. O. Roy Poulsen, Phys. Rev. C **1**, 1845 (1970).

[2] H. Hübel, R. A. Naumann, and P. K. Hopke, Phys. Rev. C **2**, 1447 (1970).

[3] Y. Y. Chu and T. E. Ward, Phys. Rev. C **8**, 422 (1973).

[4] H. Hübel, K. Freitag, E. Schoeters, R. E. Silverans, and R. A. Naumann, Phys. Rev. C **12**, 2013 (1975).

[5] T. Inamura, M. Ishihara, T. Fukuda, T. Shimoda, and H. Hiruta, Phys. Lett. **68B**, 51 (1977).

[6] D. R. Zolnowski, H. Yamada, S. E. Cala, A. C. Kahler, and T. T. Sugihara, Phys. Rev. Lett. **41**, 92 (1978).

[7] J. Wilczyński, K. Siwek-Wilczyńska, J. Van Driel, S. Gonggrijp, D. C. J. M. Hageman, R. V. F. Janssens, J. Likasiak, R. H. Siemssen, and S. Y. Van Der Werf, Nucl. Phys. **A373**, 109 (1982).

[8] T. R. McGoram, G. D. Dracoulis, A. P. Byrne, S. M. Mullins, T. Kibédi, R. A. Bark, and A. M. Baxter, Department of Nuclear Physics, Annual Report ANU-P/1381, 1998 (unpublished), p. 19.

[9] G. J. Lane, A. P. Byrne, and G. D. Dracoulis, Department of Nuclear Physics, Annual Report ANU-P/1118, 1992 (unpublished), p. 114.

[10] G. D. Dracoulis and A. P. Byrne, Department of Nuclear Physics, Annual Report ANU-P/1052, 1989 (unpublished), p. 115.

[11] K. C. Yeung, Ph.D. thesis, Australian National University/ University of Surrey, 1994 (unpublished).

[12] G. D. Dracoulis, A. P. Byrne, T. Kibédi, T. R. McGoram, and S. M. Mullins, J. Phys. G **23**, 1191 (1997).

[13] G. D. Dracoulis, S. M. Mullins, A. P. Byrne, F. G. Kondev, T. Kibédi, S. Bayer, G. J. Lane, T. R. McGoram, and P. M. Davidson, Phys. Rev. C **58**, 1444 (1998).

[14] S. M. Mullins, G. D. Dracoulis, A. P. Byrne, T. R. McGoram, S. Bayer, W. A. Seale, and F. G. Kondev, Phys. Lett. B **393**, 279 (1997).

[15] Y. Y. Chu, P. E. Haustein, and T. E. Ward, Phys. Rev. C **6**, 2259 (1972).

[16] I. H. Redmount, T. L. Khoo, and R. A. Warner, Michigan State University, Annual Report, 1974, p. 66.

[17] S. M. Mullins, A. P. Byrne, G. D. Dracoulis, T. R. McGoram, and W. A. Seale, Phys. Rev. C **58**, 831 (1998).

[18] T. L. Khoo and G. Løvhøiden, Phys. Lett. **67B**, 271 (1977).

[19] C. Baglin, Nucl. Data Sheets **72**, 617 (1994).

[20] Y. Tanaka, R. M. Steffen, E. B. Shera, W. Reuter, M. V. Hoehn, and J. D. Zumbro, Phys. Rev. Lett. **51**, 1633 (1983).

[21] M. N. Verges and R. K. Sheline, Phys. Rev. **132**, 1736 (1963).

[22] F. A. Rickey and R. K. Sheline, Phys. Rev. Lett. **17**, 1057 (1966).

[23] T. F. Thorsteinsen, G. Løhoiden, J. S. Vaggen, A. Bjornberg, and D. G. Burke, Nucl. Phys. **A363**, 205 (1981).

[24] R. Richter, I. Förster, A. Gelberg, A. M. I. Haque, P. Von Brentano, R. F. Casten, H. G. Börner, G. G. Colvin, K. Schreckenbach, G. Barreau, S. A. Kerr, H. H. Schmidt, P. Hungerford, H. J. Scheerer, T. Von Egidy, and R. Rascher, Nucl. Phys. **A499**, 221 (1989).

[25] J. C. Hill and R. A. Meyer, Phys. Rev. C **13**, 2512 (1974).

[26] P. Kleinheinz, R. F. Casten, and B. Nilsson, Nucl. Phys. **A203**, 539 (1973).

[27] F. W. de Boer, P. F. A. Goudsmit, B. J. Meijer, J. C. Kapteyn, J. Konijn, and R. Kamerans, Nucl. Phys. **A263**, 397 (1976).

[28] R. D'Alarcao, P. Chowdhury, E. H. Seabury, P. M. Walker, C. Wheldon, I. Ahmad, M. P. Carpenter, G. Hackman, R. V. F. Janssens, T. L. Khoo, C. J. Lister, D. Nisius, P. Reiter, D. Seweryniak, and I. Wiedenhoever, Phys. Rev. C **59**, R1227 (1999).

[29] H. J. Körner, F. E. Wagner, and B. D. Dunlap, Phys. Rev. Lett. **27**, 1593 (1971).

[30] H. L. Nielsen, K. Wilsky, J. Zylicz, and G. Sørensen, Nucl. Phys. **A93**, 385 (1967).

[31] T. A. Siddiqi and G. T. Emery, Phys. Rev. C **6**, 1009 (1972).

[32] F. G. Kondev, G. D. Dracoulis, A. P. Byrne, T. Kibédi, and S. Bayer, Nucl. Phys. **A617**, 91 (1997).

[33] Kiran Jain, P. M. Walker, and N. Rowley, Phys. Lett. B **322**, 27 (1994).

[34] V. G. Soloviev, Nucl. Phys. **A633**, 247 (1998).

[35] T. L. Khoo, J. C. Waddington, and M. W. Johns, Can. J. Phys. **51**, 2307 (1973).

[36] S. Nagamiya and T. Yamazaki, Phys. Rev. C **4**, 1961 (1971).

[37] Å. Bohr and B. R. Mottelson, *Nuclear Structure* (Benjamin, Reading, MA, 1975), Vol. II, pp. 45, 56, 255ff.

[38] S. Büttgenbach, M. Herschel, G. Meisel, E. Schrödl, and W. Witte, Z. Phys. A **260**, 157 (1973).

[39] I. Alfter, E. Bodenstedt, W. Knichel, J. Schüth, and R. Vianden, Z. Phys. A **355**, 363 (1996).

[40] O. Prior, F. Boehm, and S. G. Nilsson, Nucl. Phys. **A110**, 257 (1968).

[41] G. D. Dracoulis, in Proceedings of the EPS International Conference on Achievements and Perspectives in Nuclear Structure, Crete, 1999.

[42] D. M. Cullen, S. L. King, A. T. Reed, J. A. Sampson, P. M. Walker, C. Wheldon, F. Xu, G. D. Dracoulis, I.-Y. Lee, A. O. Macchiavelli, R. W. Macleod, A. N. Wilson, and C. Barton, Phys. Rev. C **60**, 064301 (1999).

[43] G. D. Dracoulis, F. G. Kondev, and P. M. Walker, Phys. Lett. B **419**, 7 (1998).

[44] D. C. Radford, Nucl. Instrum. Methods Phys. Res. A **306**, 297 (1995).